Extended Abstracts of the 1993 International Conference on Solid State Devices and Materials, Makuhari, 1993, pp. 724-726 **PD-2-8**

Reverse Characteristics Analysis of Different AlInAs-Schottky Contacts

H. Hoenow, H.-G. Bach*, and G. Heymann

Humboldt-Universität zu Berlin, Inst. für Werkstoffe und Verfahrenstechnik
Invalidenstr. 110, D-10099 Berlin, FRG
*Heinrich-Hertz-Institut für Nachrichtentechnik Berlin GmbH
Einsteinufer 37, D-10587 Berlin , FRG

We present a study of I-V and C-V characteristics on metal-semiconductor contacts on $Al_{0.48}In_{0.52}As$ comparing different preparation techniques. The merit of barrier analyses by C-V and I-V measurements is increased by considering temperature effects, thus clarifying technology related effects on metal-semiconductor interfaces. We relate detected differences between I-V- and C-V-derived barrier heights to plasma-based technology induced defects. Furthermore we identified additional reverse current contributions in AlInAs-Schottky diodes by temperature resolved I-V current characteristics in conjunction with simulations.

1. Introduction

AlInAs layers are applied in many device structures as barrier material for high quality Schottky contacts e.g. in HEMT's and MSM diodes. The quality of this metal-semiconductor junction has a great impact on the device parameters and reliability. Different contact metallizations and surface cleaning procedures are discussed in the literature /2,3/.

The parameters barrier height Φ_b (from I-V or C-V measurements) and ideality factor n are usually taken to characterize the Schottky contacts. We show that these two parameters are insufficient to characterize the metal-semiconductor interface, especially under reverse-field aspects. A clear distinction between I-V and C-V calculated barrier heights is required for more detailed analyses. Many different effects must be taken into account particularly in the case of high reverse bias /1/.

We report on a study of Schottky contacts made on MBE grown AlInAs:Si layers with different metallization systems, surface pretreatments and deposition technologies. We characterize the Schottky barriers with C-V-, forward and reverse I-V-, and temperature resolved reverse I-V-measurements.

2. Sample fabrication

AlInAs layers were grown on epi-ready (100)-oriented InP:S substrates by MBE. A Si doping concentration of $8*10^{16}cm^{-3}$ with horizontal doping profile determined by capacitance versus voltage measurements was incorporated into the AlInAs layers of 1 µm thickness. A conventional lift-off procedure is used to separate the Schottky devices after metal evaporation. Ohmic contacts were realized on the back side of the substrate with a sputtering process of 50 nm Ti and 200 nm Au after Ar-ion plasma etching of the surface with 500 V accelerator voltage.

In order to optimize the Schottky contacts on AlInAs we have investigated the following technological steps: wet etching surface pretreatment, in-situ (in an UHV evaporation system) Ar^+-ion beam etching, different metallization layers and deposition technologies. As metallization systems we used Ti/Pt/Au as well as Pt/Ti/Pt/Au, the latter offering the potential of higher Schottky barriers, furthermore the seldom used metals W/Ti/Au, Pd/Ti/Pt/Au and additionally Au contact as reference. Further on we fabricated some of the above mentioned metallizations with different deposition technologies, pure e^--beam evaporation, Ar^+-ion etching before e^--beam evaporation and a sputter deposition of the first metal layers (Pt/Ti, Ti, W/Ti, Au).

3. Results and evaluation procedures

At first we investigated the influence of a wet chemical etching pretreatment of the AlInAs surface by Pt/Ti/Pt/Au (5/20/50/200 nm) EBEV (electron beam evaporation) metallization. The HF-Dip (HF : H_2O / 1 : 1000) with an etching time of 10 s offered the best results with respect to the barrier height Φ_{bn} with minimum standard deviation $\sigma_{\Phi b}$. Fig. 1 shows the forward I-V characteristics of evaporated Schottky contacts obtained with different metallization systems. The semi-log plots exhibit good linear characteristics over 3 decades for Ti/- and Pd/-metallization systems and 6 decades for the Pt/Ti/Pt/Au sequence. Pt-based contacts yield the highest barrier heights, an ideality factor of n=1.1 (see table 1) and sufficient homogeneity. These results are in agreement with data from /2,3/.

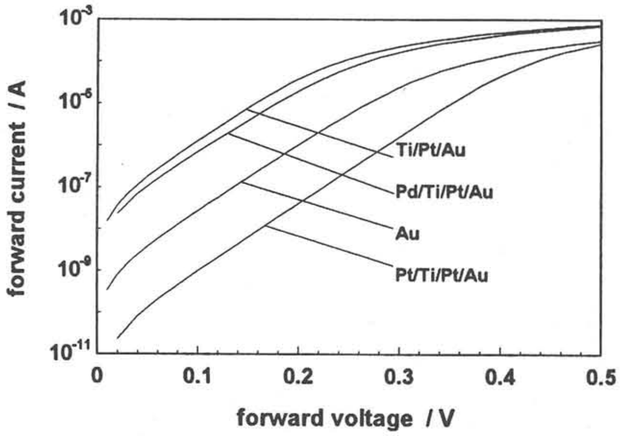

Fig. 1 Forward I-V characteristics of AlInAs Schottky diodes; e^--beam evaporation of different metal sequences

Data for barrier heights (C-V and I-V) and ideality factors are summarized in table 1.

metal sequences	$n \pm \sigma_n$	$\Phi_{bn}^{(I-V)} \pm \sigma_{\Phi b}$ / eV	$\Phi_{bn}^{(C-V)}$ / eV
EBEV			
Ti/Pt/Au	1.09 ±0.02	0.590 ±0.013	0.66
Au	1.12 ±0.01	0.678 ±0.005	0.76
Pd/Ti/Pt/Au	1.11 ±0.02	0.588 ±0.007	0.7
Pt/Ti/Pt/Au	1.10 ±0.04	0.74 ±0.02	0.77
Pt/Ti/Pt/Au[1)]	1.10 ±0.02	0.648 ±0.003	0.82
plasma sputtering			
Ti/Pt/Au	1.20 ±0.002	0.614 ±0.002	1.1
Pt/Ti/Pt/Au	1.07 ±0.01	0.714 ±0.002	1.05

Table 1 Extracted I-V and C-V barrier parameters of investigated Schottky diodes;
[1)] Ar-etched sample

The smaller standard deviation for Φ_{bn} and n of the Ar-etched and sputtered samples is obvious which correlates with a high uniformity of the Schottky contacts. The deviation between I-V- and C-V-determined barrier heights is also visible for most of the samples in table 1. The influence of pretreatment and deposition technology on the I-V and C-V deduced barrier heights are shown in Fig. 2. An increase of the deviation between both barrier values is visible for Ar-etching and sputtering technologies. Fig. 3 shows the C-V curves and $1/C^2$ plots of Pt-based Schottky contacts obtained with different deposition technologies on the same AlInAs layer. A decrease of the capacitance or positive bias shift of the complete C-V curve is visible for the Ar-etched and even more for the sputtered contacts. Both interpretations will lead to an artificial increase of the $1/C^2$ x-axis intercept, which usually represents the built-in voltage and delivers the C-V barrier height, see table 1.

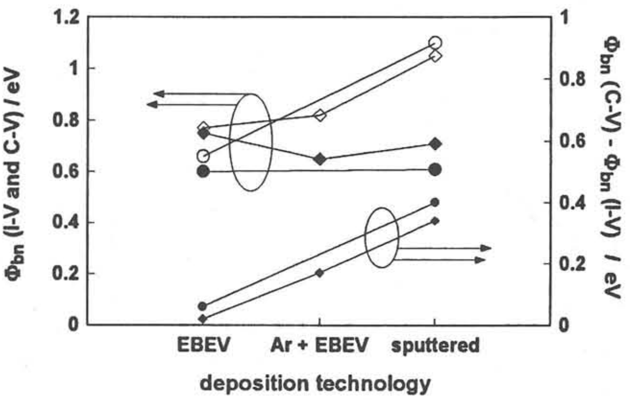

Fig.2 Barrier heights of contacts obtained with different technologies,
circles:Ti/Pt/Au; squares:Pt/Ti/Pt/Au;
filled symbols: I-V data, open: C-V data

For small differences models of thin interface layers /2,4/ or potential fluctuations /5/ were often discussed. The samples fabricated with Ar^+-ion beam etching or sputter deposition technology show a remarkable difference in C-V and I-V extracted barrier heights up to 400 meV. The existence of intervening layers of oxide and other contamination is notably excluded for Ar^+-beam technology. We assume damaged surface layers and incorporated charges, induced by high-energy surface preparation and deposition technologies to explain these C-V deviations.

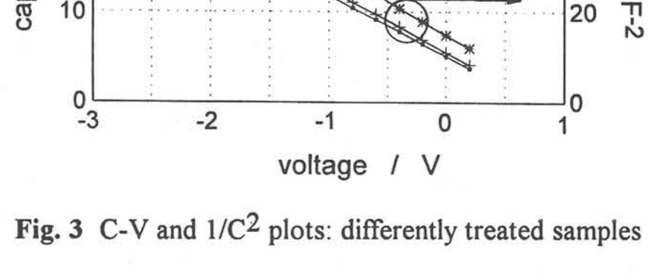

Fig. 3 C-V and $1/C^2$ plots: differently treated samples

Results from temperature dependent reverse I-V measurements (described later) verify the I-V barrier height as carrier transport limiting according to equ. 1 /1/ in contrast to the charge-control related barrier evaluation within the C-V method. The high-energy surface preparation and deposition technologies Ar-beam etching and plasma sputtering are supposed to convert a very thin surface sheet of the AlInAs layer into a carrier depleted or even more into a highly (negative) charged surface layer (N_{sheet} up to |-$2 \cdot 10^{13}$ cm^{-2} |). The damaged region may be assumed only within the first nm of the structure, estimated from the Ar-ion and Ti atomic mass and highest available accelerating energies in the keV regime. Such thin surface layers, based on transformed AlInAs material, will be transparent for tunneling electron transport. Nevertheless these surface layers will carry a considerable potential drop, which adds onto the parabolic band diagram of the underlying undisturbed AlInAs layer. If highly *negative* charged surface layers would be sufficiently *thick* (>10nm), compared to the electron tunneling length (5nm), these layers would work like p-type doped surface layers for barrier enhancement purposes, described e.g. in /6/. However, in the actual samples the additional potential contribution detected by the C-V method can not be exploited for barrier enhancement due to electron tunneling, as indicated by the I_F-V deduced effective barrier values given in table 1.

$$J = A^{**}T^2 \exp(-\frac{q\phi_{bn}}{kT})*(\exp(\frac{qV}{nkT}) - 1) \qquad (1)$$

with

$$q\phi_{bn} = q\phi_{b0} - q\Delta\phi - q(\Delta\phi)_{static}$$
$$\text{and } q(\Delta\phi)_{static} = \alpha\,\vec{E} \qquad (2)$$

Furthermore, we made temperature resolved reverse I-V measurements and used simulations (equ. 1,2) to identify the reverse-field behaviour of the barrier height Φ_b. Fig. 4 shows a set of typical measured curves and related simulation results. A comparison of simulation data based on extracted barrier heights verifies the assumption that the I-V deduced value for Φ_b presents the thermal emission properties of the transport mechanism over the barrier. The reverse characteristics of AlInAs-Schottky contacts show two regions with different dominating current mechanisms. For a reverse bias range from 1 to 6 V a clearly field dependent barrier lowering is detected, characterized by the alpha factor $q(\Delta\phi_b)_{static} = \alpha * \vec{E}$ in equ. 2 /1/, representing an additional linear electric field lowering of Φ_{bn} in addition to the intrinsic image force lowering $\Delta\Phi$. For higher reverse voltages (6-10V) we found a tunneling transport mechanism. These tunneling currents are observed at contacts from all metallization systems, pretreatment variations, and deposition technologies and its magnitude is relatively independent from the Schottky barrier height. This indicates a material related mechanism, tunneling through the conduction band barrier spike seems likely.

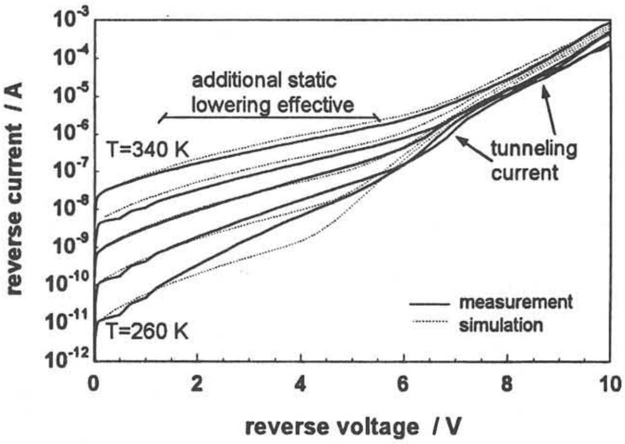

Fig. 4 Reverse current characteristics of an Ar-etched Pt/Ti/Pt/Au Schottky contact, T-step 20K

4. Summary

Although Ar^+-ion beam pretreated Schottky diodes offer better barrier uniformity, a well controlled wet chemical pretreatment of the AlInAs surface should be preferred with respect to the highest obtainable barrier height (Φ_{bn}=0.74 eV at $8*10^{16}cm^{-3}$ doping level). Plasma based cleaning and metal deposition technologies tend to damage the AlInAs surface within the first nm of the surface, which can be detected by C-V analyses compared to barrier heights from I-V curves.

More or less slightly damaged Schottky barriers on AlInAs show an additional linear electric-field dependent barrier-lowering mechanism, according to the potential bending sensitivity of the thin surface region. Tunneling currents contribute to the reverse leakage at surface electrical field strengths exceeding ≈ 400 kV/cm. These results give a sounder understanding of barrier characterization and reverse current mechanisms in devices with AlInAs-barrier layers.

Acknowledgement

The authors like to thank Mrs. J. Böttcher for MBE growth, A. Umbach and Mrs. M. Arbert for technological help and P. Harde for valuable discussions.

References

/1/ S. M. Sze, Physics of Semiconductor Devices, John Wiley & Sons, New York, Second Edition (1981) 254.

/2/ L.P. Sadwick, C.W. Kim, K.L. Tan, and D.C. Streit: IEEE Electron Device Lett. **12** (1991) 626.

/3/ N. Harada, S. Kuroda, and K. Hikosaka: IEICE Trans. Electron. **E75-C** (1992) 1165.

/4/ C. Schramm, H.-G. Bach, H. Künzel, and J.P. Praseuth: J. Electrochem. Soc. **138** (1991) 2808.

/5/ J.-H. Werner and H.-H. Güttler: J. Appl. Phys. **69** (3) (1991) 1522.

/6/ S.V. Averin, A. Kohl, R. Müller, J. Wisser, and K. Heime: Solid-State Electron. **36** (1) (1993) 61.